

STUDY OF COMPRESSION-RELATED LUMBAR SPINE FRACTURE CRITERIA USING A FULL BODY FE HUMAN MODEL

Ning Zhang

Jay Zhao

Takata (TK Holdings)

United States

Paper Number 13-0288

ABSTRACT

A detailed lumbar spine FE component model (including vertebrae, inter-vertebral discs, all ligaments and facet joints of T12-L5) was built per the Global Human Body Model Consortium (GHBMC) CAD data. The lumbar model was correlated with the Post-Mortem Human Subject (PMHS) lumbar spine tests under flexion, compression and anterior shear loading modes in the physiological ranges (Belwadi, 2008), and was validated with the tests of PMHS functional spine units (FSU) of three adjunct vertebrae in fracture loading conditions (Belwadi, 2008). The lumbar model was integrated into the Takata in-house 50th percentile full human body model. The full body model was validated with the Wayne State University (WSU) PMHS vertical sled tests under +Gz loading in the range of 6G to 10G (Prasad, 1973). Good agreements were found between the test results and the FE model. At the lumbar component levels, stiffness and failure loads along with failure modes were correlated. At the full body level, the seat pan load cell forces, intra-vertebral body force, and the tissue level strains along superior-inferior direction at the anterior vertebral shells were correlated.

Using the validated human model, impactor tests were simulated for a mid-sized human male lying on a table in a vertically sitting posture impacted with a 44kg impactor of 300mmX300mm size onto the buttocks and thigh area at multiple impact speeds from 5.8 m/s to 15 m/s. The simulation results showed that the threshold impactor speeds (or energies) at which the human lumbar vertebrae fractures at the L1 level occurred were in the range of 8.92-10.6m/s (or 1750-2475J impact energy), varying with the fracture type and the test set up conditions.

Physical lab impactor tests in the same test setup configuration were run for the H3 50th%ile dummy at multiple impact speeds in the range of 5.8m/s-7.5m/s. The test data showed that the

dummy lumbar load Fz reached 14.5 KN at the 7.5m/s impact.

INTRODUCTION

Compression-related spine fractures are often observed in frontal crashes. Recent studies using the NASS database showed an increase in incidence of thoraco-lumbar fractures in vehicles from later model years. (Pintar, 2012a). Jakobsson et. al. (2006) surveyed 189 vertebral fracture cases from a sub set of 21,034 Volvo car accidents database between 1995 and 2005. The data showed a significantly reduced injury risk for MAIS 2+ cases when comparing the 1995-1999 older cars with 2001-2005 newer cars, however, an insignificant reduction in AIS 2+ vertebral fractures was found between older car groups and newer car groups.

At the lumbar tissue and component test level, there have been numerous published studies on the PMHS lumbar spine response and fracture tolerance under different laboratory test conditions. The tissue test data for the vertebral bodies, ligaments and discs were reported (Yoganandan et al. 1988a). Stiffness and strength of the lumbar spine were experimentally studied using two or three adjacent lumbar vertebrae called the Functional Spine Unit (FSU) (Yoganandan et al. 1988b, Ashton-Miller and Schultz, 1997, A. Belwadi et al., 2008) subjected to a single loading mode such as anterior shear, flexion, and compression, or combined loadings. Whole lumbar spine tests were also performed. (Demetropoulos et al, 1998, A. Belwadi et al, 2008). The reported FSU compression tests showed that the wedge compression fracture (fx) occurred at the failure forces in the range of 2-5KN of the lumbar force, the vertebral body fx observed at 4.3-5.6KN, and the end-plate fx at 5.6-10.2KN.

At the whole PMHS test level, however, there have been relatively few published lumbar injury studies. In earlier 1970s studies whole body PMHS

were applied vertical loading with a vertical sled to simulate pilot ejection forces (King and Vulcan 1971). Recently, a few whole body PMHS were applied underbody loading with a Hyge sled in a high G, short time duration pulse to investigate the blast effect on the lumbar injuries (Pintar, 2012b). Nevertheless, compression-related spine fracture mechanisms of the full human body in various motor vehicle crash conditions were not fully understood. There were no sufficient whole PMHS lumbar testing data for use to derive risk functions of compression-related spine fractures. Also comparative experimental studies for PMHS and Anthropomorphic Test Dummies (ATDs) on the lumbar injury measures and the associated tolerances were rarely seen in literature. Therefore, there was no agreed tolerance for assessment of lumbar spine fractures in motor vehicle safety standards. This situation adversely affected to some extent development of advanced restraints for mitigating risk of the lumbar injuries.

To address this issue, we were motivated firstly to develop a viable lumbar injury assessment tool, and then to develop a simple pendulum impact lab test protocol, to study the lumbar injuries of full human bodies subjected to compression dominated loadings. Such defined physical tests for an ATD like the Hybrid-III 50thtile dummy, combined with the test simulations using a validated mid-sized human body model, should help us better understand the human lumbar vertebrae fracture tolerances and the corresponding injury measure reference values of the Hybrid-III dummy for the test conditions.

The objectives of this study were

- 1) to develop the human lumbar fracture criteria of a mid-sized male human model;
- 2) to determine the threshold impactor speeds (or energies) for an impactor test configuration at which the human lumbar vertebrae fractures at L1 level occurred;
- 3) to estimate the lumbar fracture research reference values for the H3 50thtile dummy corresponding to the threshold impactor speeds through comparative study of the lumbar loads between the Hybrid-III 50thtile dummy and the human model.

METHODS

The first part of this study was to develop a mid-sized male human body model capable of

predicting the lumbar injury patterns. Secondly, with this validated model, a series of impactor tests applied to the underbody of the human body were to be simulated. Correspondingly, physical laboratory impactor testing for the Hybrid-III 50thtile dummy would be run. Finally, analyses were made to define at what threshold impact test conditions injuries to the human lumbar spine would likely occur, and correspondingly what were the corresponding lumbar loads of the Hybrid-III dummy. A lumbar fracture research reference value for the H3 50thtile dummy could be derived via this approach.

Full human body model upgrade

A previously validated Takata in-house full human body model (Zhao and Narwani, 2007) was further developed for this study. The upgraded model (named as TKHM v4.0) was integrated with the latest developed refined body region models of the thorax, the shoulder and upper extremities, the abdomen, and the pelvis. These body region models were constructed with more accurate anthropometry data and refined meshes of elements with higher standard of meshing quality. The PMHS validation test protocols previously used for these body regions of the human model (Zhao and Narwani, 2007) were re-performed for TKHM v4.0. Additional model validations against recently published component and whole PMHS tests were conducted, which included UVA Rib segment bending tests, isolated rib ring loading tests, point loading to isolated ribcage (Kindig, et al., 2010), and restrained PMHS in frontal sled tests (Shaw, 2009). All the validations demonstrated that the upgrade full body model had improved robustness and kinematics; the refined body region models had better biofidelic responses than the previous version as well.

Modeling of Lumbar spine

Next, a more biofidelic lumbar spine FE component model was developed. A detailed lumbar spine model including vertebrae, inter-vertebral discs, all ligaments and facet joints of T12-L5 was built per GHBMC CAD data representing a healthy young adult male in the driving posture. The vertebrae (body and posterior structure) and inter-vertebral discs were meshed with hexahedra elements of high element quality. Cortical shells wrapped around vertebrae were modeled as shell elements sharing nodes with the surface of solid elements. The anterior longitudinal ligament, the posterior longitudinal ligament, and the interspinous ligament were modeled with membrane elements of specified thickness.

Contacts on facet joints between adjacent vertebrae were defined and surrounding facet capsules were modeled with membrane elements.

Based on the geometrically symmetrical condition, half of spine was built first. It was used for component level validations. The whole lumbar model was built from it using mesh reflection along the symmetric plane. The lumbar model was later assembled into the full human body model (TKHM v4.0) with nodal connections to adjacent connective soft tissue parts (representing muscle and fat).

Material properties of lumbar spine model

Material laws and input parameters for all lumbar components were carefully selected according to the biological tissue’s material behavior under both physiological and pathological loadings of laboratory measurements documented in literature. For the trabecular bone inside vertebral body and the cortical bones surrounding the vertebrae, an elastic-plastic material law was selected to consider the fracture failure of tissues under high loading levels (See Table 1 and 2). For the soft tissues, the ligaments were represented as fabric type of material with no resistance for compressive force. The Annulus fibrous was model as elastic, and the nucleus was modeled as fluid type of material with incompressible property (See Table 3 and 4).

Table 1.

Input material parameters for cortical bone

Thickness (mm)	0.36
Density (kg/liter)	1.4
Elastic modulus (GPa)	17.0
Poisson’s ratio	0.3
Yield stress (MPa)	133
Strain at failure (%)	0.89
Tangent modulus (MPa)	230

Table 2.

Input material parameters for trabecular bone

Density (kg/liter)	0.9
Elastic modulus (GPa)	0.062
Poisson’s ratio	0.3
Yield stress (MPa)	3.2
Strain at failure	24%

Table 3.

Input material parameters for ligaments

Density (kg/liter)	1.1
Elastic modulus (GPa)	0.013
Poisson’s ratio	0.4

Table 4.

Input material parameters for inter-vertebral disc

Density (kg/liter)	1.3
Elastic modulus (GPa)	0.029
Poisson’s ratio	0.45

Component validations

The lumbar model was subjected to compressive, flexion and anterior shear loading separately according to the laboratory setup using whole lumbar specimens (Demetropoulos, 1998, A. Belwadi, 2008). The loading levels for these tests were within the lumbar spine’s physiological loading range without damaging any of the tissues. The loading rate in the simulation was carefully selected to make sure that dynamic effects were negligible.

According to the test setup, the lumbar spine including S1 and T12 was mounted upside down, and vertebra S1 were potted into a fixed jig, and vertebra T12 was potted into a jig whose actuator applied a displacement-controlled loading. A six-axis loadcell was connected to the fixed jig on the S1 side. The model setup followed the test setup, and the aluminum potting cups at both ends were modeled as rigid. Prescribed motion boundary conditions were applied to the cup at the T12 side; the loadcell at the S1 side was modeled using a zero beam loadcell element to output the forces and moments. Table 5 shows the loading level for each loading mode. Figure 1 shows the model setup.

Table 5.

Applied loading type and jig motion

Loading type	Jig motion
Compressive	3.5 mm
Anterior shear	18 mm
Flexion	9 degrees

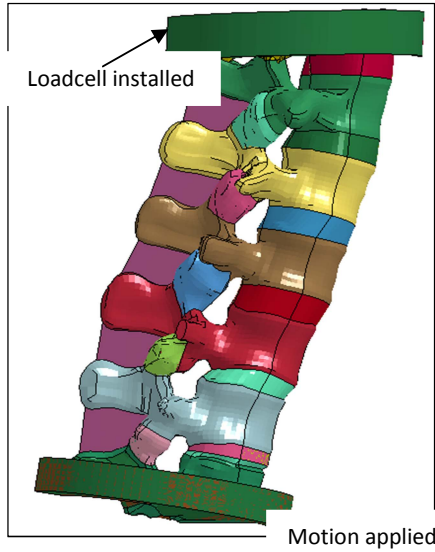


Figure 1. Lumbar spine static loading model setup.

A three segment FSU model including L4, L5, and S1 (See Figure 2) was studied at the component level to verify the material failure criteria for both vertebral cortical shell and trabecular bone exceeding the fracture loading level. Two loading modes: a 10mm compressive displacement, and a combined loading consisting of 15mm shear and 9 degrees of flexion (Belwadi, 2008) were simulated and the failure load was reported and compared with the reported laboratory tests.

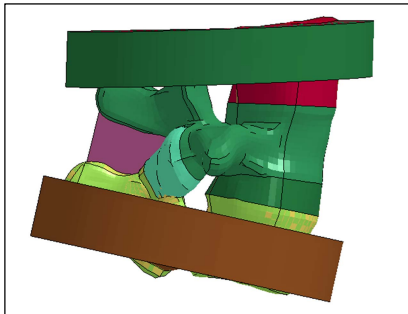


Figure 2. Lumbar functional spine unit (FSU) failure test model setup.

Full body model validation under vertical sled loading

The full body model integrated with the validated lumbar sub-model was further validated against the PMHS tests in a vertical sled system (King and Vulcan, 1971). Figure 3 shows the model setup. The human model was positioned in a vertical sitting posture and restrained with a four point seat belt system with an 180N pretension load. Several vertical acceleration pulses were applied to the seat

and foot rest experienced peak acceleration levels varied from 6g to 10g according to the tests. The seat pan-pelvis contact force, lumbar loadcell output, and strain outputs on the anterior vertebral body at the L1 and L3 level were correlated with PMHS test results. Since the instrumentation was different for every test, 3 cases were selected and listed in Table 6.

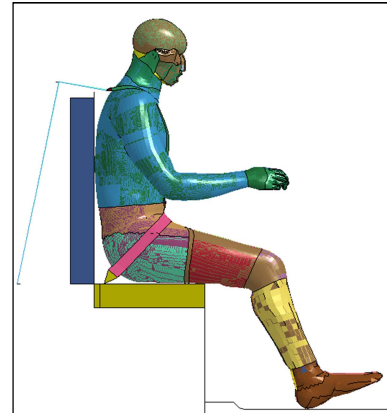


Figure 3. Full body human model validation setup according to test protocol from King and Vulcan, (1971).

Table 6.
Cases used to validate the full human body model

Source of data	Peak G Sled pulse	Instrumentation
King and Vulcan, 1971	10G	L1, L3 strain gage
Prasad, 1973	8G	Lumbar vertebral load cell
Prasad, 1973	6G	Seat pan load cell

Human body underbody impact tests simulation

A linear impactor test configuration for the underbody of the human body was defined, as shown in Figure 4. The validated full human body model was positioned lying on a wood table in a vertically sitting posture. A foam block of small weight (109g) was put underneath his head to hold the head initial position. The height of the impactor was positioned aligned with the center of pelvis of human model. The weight of impactor was 44kg, and the dimension was 300mmx300mm square with a D-shape cross section on the impact side.

Eleven test simulations (Table 7) were initially simulated, with an initial pendulum impact velocity starting at 5.8m/s which was gradually increased to 15m/s step by step to find the velocity level at which the lumbar vertebrae would start to fail.

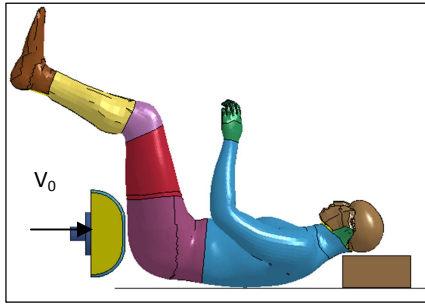


Figure 4. Linear Impactor test setup for the full human body model.

Table 7.
Lists of cases of the human model impactor simulations.

Case #	Impactor Velocity (m/s)	Impactor kinetic energy (J)
1	5.8	740
2	6.5	929
3	7.5	1237
4	8.3	1500
5	9.5	2000
6	10.6	2500
7	11.7	3000
8	12.6	3500
9	13.5	4000
10	14.3	4500
11	15	5000

Hybrid III 50th underbody linear impactor testing

A laboratory study using a Hybrid-III 50th percentile dummy was conducted following the same impactor test configuration for the full human body model. The dummy was instrumented with a 6-axis lumbar spine load cell (model 4609JTF, Humanetics, Plymouth, MI) with a capacity of 20KN for force and 600Nm for moment measurement. Due to the limitation of the linear impactor system, the maximum velocity the system could achieve was 7.5m/s. Several dummy positions were tested to investigate the effect of the pelvis/lumbar angle. Table 8 showed the test matrix. Figure 5 showed the test setup. The dummy output included: head acceleration, chest acceleration, pelvis acceleration, and lumbar forces and moments. All signals were processed according to the SAE J211 standard.

Table 8.
Test matrix of H3 50% laboratory linear impactor test.

Test number	Impactor velocity	Pelvis angle
-------------	-------------------	--------------

	(m/s)	(degrees)
1	5.8	0
2	5.8	15
3	5.8	20
4	5.8	25
5	6.5	0
6	6.5	25
7	7.5	0
8	7.5	25



Figure 5. Linear impactor setup for the H3 50thtile dummy

RESULTS

Results of lumbar model under physiological range of static loading

The load-deflection curves were plotted and linear curve fitting was used to calculate the stiffness of the lumbar model under compression, anterior shear and flexion. Figure 6 (a-c) show the model predictions against the test results for the PMHS lumbar spine specimens. For all three loading modes, lumbar stiffness predictions were within the range of test data variations.

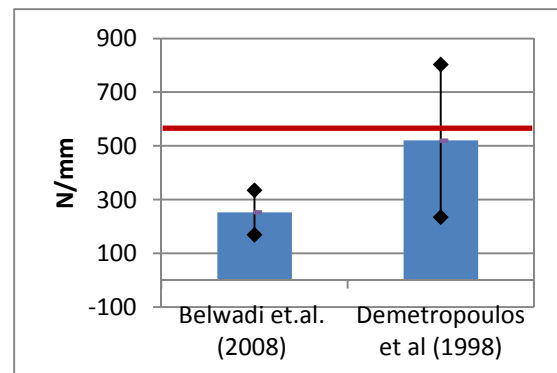


Figure 6(a). Compressive stiffness of lumbar spine (L1-L5), flat red line was the model prediction.

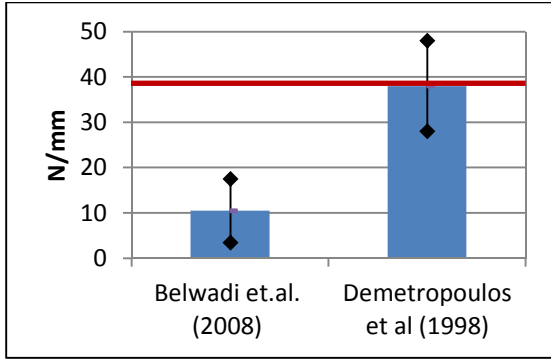


Figure 6(b). Anterior shear stiffness of lumbar spine (L1-L5), flat red line was the model prediction.

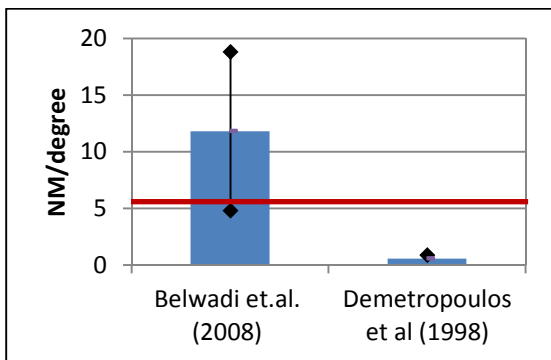


Figure 6(c). Flexion stiffness of lumbar spine (L1-L5), flat red line was the model prediction.

Results of failure loading cases with FSU model

When the pure compressive force was applied to the FSU model, a compression fracture of the vertebral body was predicted (Figure 7). The predicted failure force was 6.3 KN. Figure 8 compares the model predicted compressive failure force with the data of FSU tests under the pure compression conducted by Baudrit (2005) et al. The tests showed that a failure force of 10.2 ± 1.71 KN for young specimens (age: 22-46, male) and 5.58 ± 1.64 KN for elderly specimens (age: 46+, male and female), the result from this study was within the range of the elderly group. When the combined shear and flexion load was applied, a posterior structure failure was predicted for the vertebrae (Figure 9). The failure force vs. failure moment (Figure 10) were plotted and compared with the PMHS tests conducted by Belwadi et al (2008). The failure load predicted by the current model was in line with the test results.

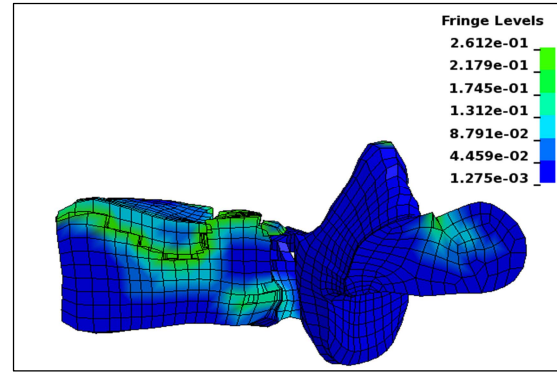


Figure 7. Predicted failure mode (compression type) for the FSU model under pure compressive force; the contour shows the effective strain.

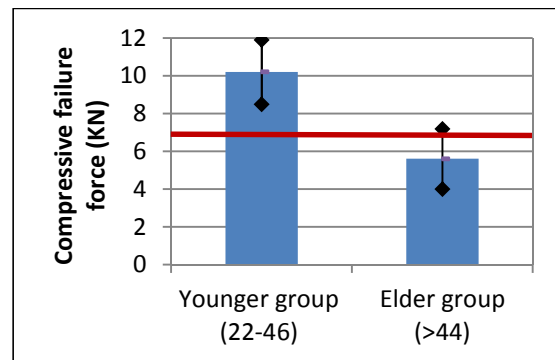


Figure 8. Predicted compressive failure compared with test data conducted by Baudrit et al. (2005). Flat red line was the model prediction.

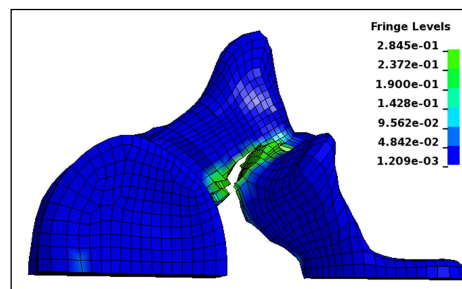


Figure 9. Predicted failure mode (posterior structure failure) for the FSU model under shear force and flexion moment (the contour shows the effective strain).

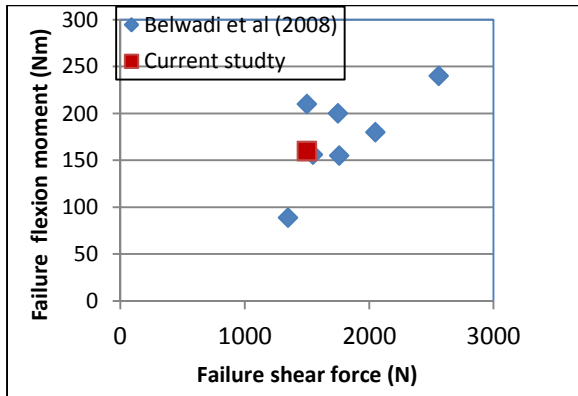


Figure 10. Predicted failure force and moment for the FSU model under shear force and flexion moment.

Results of full body validation under vertical sled loading

Good correlation was found between the model prediction and the test data (King and Vulcan, 1971) for seat pan pelvis contact force (See Figure 11). The current model slightly (13%) under-predicted the spine load Fz (See Figure 12). For the strain outputs at the anterior surface along the superior-inferior direction, the current model had good correlation for the L1 surface strain, but slightly under-predicted the first spike for the L3 vertebra (See figure 13 and 14).

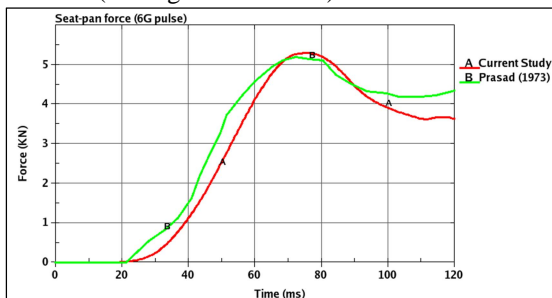


Figure 11. Comparison between the PMHS test and the simulation for seat-pan contact force.

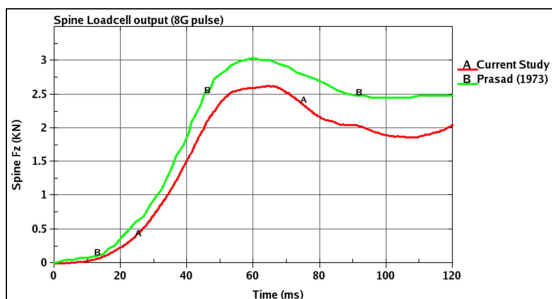


Figure 12. Comparison between the PMHS spine Fz.

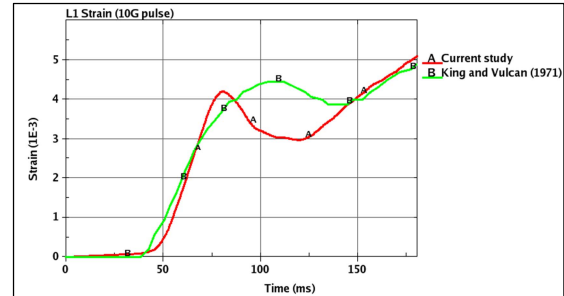


Figure 13. Comparison between the PMHS test and the simulation for strains at the L1 level.

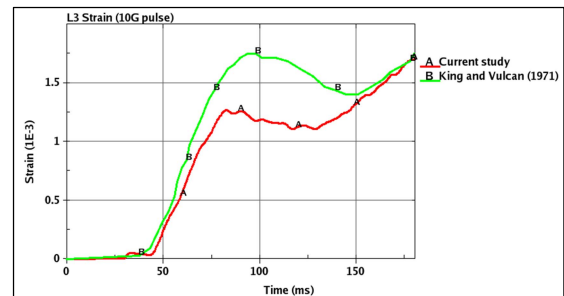


Figure 14. Comparison between the PMHS test and the simulation for strains at the L3 level.

Results of human body underbody impact tests simulations

The impact loading on the pelvis yields a dominant compressive force on the lumbar vertebrae. As a result, the L1 vertebra reported highest strain among the five lumbar vertebrae, due to the curvature of the spine (Lordosis in lumbar region). With an increase in impact velocity, both peak lumbar Fz and peak vertebral strains increased (see Table 9). At the impact speed of 10.6m/s (2475J), a wedge type fracture was observed at the L1 level (Figure 15).

Table 9.

The human model impactor simulation Results: the peak lumbar Fz, the peak vertebral strain and wedge type fracture observation.

Case #	Velocity (m/s)	Peak lumbar Fz (kN)	Peak vertebral strain (%)	Fractures observed
1	5.8	2.85	0.38	No
2	6.5	3.46	0.45	No
3	7.5	3.98	0.52	No
4	8.3	4.87	0.58	No
5	9.5	5.43	0.69	No
6	10.6	6.26	0.73	Yes
7	11.7	7.1	0.73	Yes

8	12.6	7.7	0.73	Yes
9	13.5	8.4	0.73	Yes
10	14.3	8.9	0.73	Yes
11	15	9.26	0.74	Yes

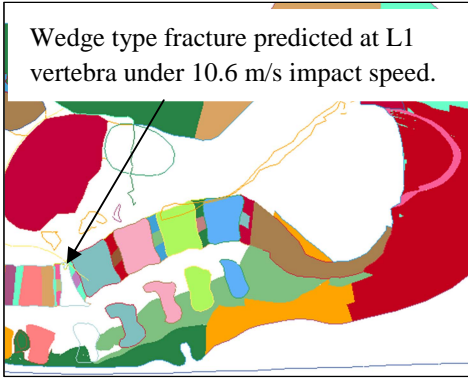


Figure 15. Cross section cut showed wedge type fracture at the L1 level for the 10.6m/s impactor simulation.

Results of Hybrid III 50th underbody linear impactor testing

Eight impacts were conducted for a H3 50th percentile dummy. Table 10 shows the measured peak lumbar Fz, My and pelvis acceleration Gz. Overall the peak lumbar Fz increased when the impact velocity increased (see Figure 16). However, the lumbar flexion moment My (positive My) was not sensitive to an impact velocity change (see Figure 17). When the dummy pelvis angle increased from 0 degree to 25 degrees, a decrease in the lumbar Fz and an increase in the lumbar extension My were observed (see Figure 18 and 19).

Table 10.

The HB3 50th%tile dummy test results: the peak values of lumbar Fz, My and pelvis Gz.

	Pelvis angle	Velocity (m/s)	Lumbar Fz (N)	Lumbar My(Nm)	Pelvis Gz (G)
1	0	5.8	8689	53	255
2	15	5.8	6229	57	136
3	20	5.8	6050	65	238
4	25	5.8	6624	52	139
5	0	6.5	12,640	44	652
6	20	6.5	6988	70	350
7	0	7.5	14,530	60	659
8	20	7.5	8785	67	533

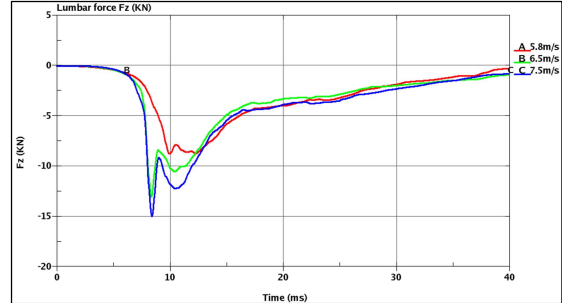


Figure 16. Comparison of the lumbar Fz forces from the tests with different impact velocities (pelvis angle was 0 for all cases).

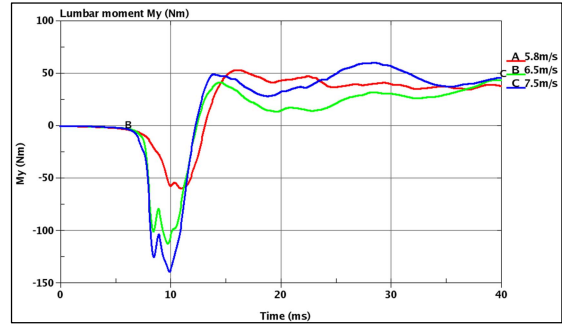


Figure 17. Comparison of the lumbar flexion moments My from the tests with different impact velocities (pelvis angle was 0 for all cases).

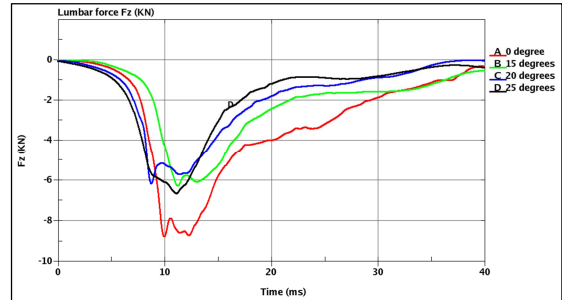


Figure 18. Comparison of the lumbar forces Fz from the tests with different pelvis angles (impact velocity was 5.8m/s for all cases).

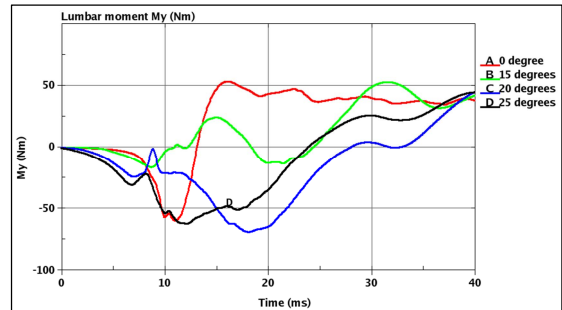


Figure 19. Comparison of the lumbar flexion moments My from the tests with different pelvis angles (impact velocity was 5.8m/s for all cases).

DISCUSSIONS

On results of component validation

For compressive and shear stiffness of the lumbar spine, the current model prediction was closer to the test data from Demetropoulos et al. (1998) than the data from Belwadi et al (2008). When looking into the PMHS' age and sex (Table 11), the specimens from Demetropoulos et al. (1998)'s study were closer to what the current model represented, which was a middle aged 50th percentile male subject. For flexion stiffness, since the testing was sensitive to initial spine positions, larger variations were observed between the two groups and the current model prediction were within the range of data reported from the above two studies.

Table 11.
PMHS statistics for lumbar spine stiffness data
from literature [Demetropoulos et al. 1998,
Belwadi et al 2008]

	Demetropoulos et al. 1998	Belwadi et. al. 2008
Number of specimens	10	7
Male/Female	8/2	6/1
Range of age	54-65	48-83
Average age	60	68
Average weight (kg)	73	75

On vertebral fracture pattern prediction

The fracture type and pattern of the vertebrae depend on the forces and moments applied to the spine (Nahum and Melvin, 1993). Compression fractures are due to the vertebrae subjected to pure compressive forces which cause the endplate to collapse and the vertebral body to compress. The failure pattern for the FSU model of the current study under the compressive force matched this type of fracture pattern. The mechanism of posterior fracture is due to excessive flexion moments causing failure of the posterior structures or ligaments and discs. The failure pattern predicted by the FSU under flexion and anterior shear matched this type of fracture. A combination of flexion and axial compression causing excessive compression at the anterior site of the vertebral body results in anterior wedge fractures. The loading of the full human body when subjected to underbody impactor loading was a compression dominated force with additional flexion moment caused by the spine curvature around the lumbar and thoracic spine transition zone. Therefore, the

wedge fracture predicted from the full body impactor model is reasonable.

On Hybrid III 50th percentile dummy lumbar fracture research reference value and bio-fidelity

The test data (Table 10) showed that the dummy lumbar load Fz reached 14.5 KN at the 7.5m/s impact. A simple linear aggression and interpolation of the data set could be made. It was estimated that about 15-16KN of the dummy lumbar load Fz could be generated at the threshold impact speed of 8.92m/s (see next discussion). The lumbar fracture research reference value for the H3 50th percentile dummy subjected to compressive dominant impact loadings could be in this range. This needs further experimental verification.

Hybrid III family dummies (Backaitis and Mertz, 1994) are widely used for automotive safety design and biomechanical research. However, there are several limitations to directly apply the H3 dummy as a surrogate for lumbar spine injury study and prevention. First, the curvature of the lumbar spine of the H3 dummy is in Kyphosis instead of Lordosis which is the characteristic of the human spine. The curvature differences make the moment measurement at the lumbar spine loadcell less accurate compared with the moment sustained by the human spine. Figure 20 shows a direct comparison of the lumbar moment output at 7.5 m/s impact speed between the human model prediction and the Hybrid III dummy. The dummy exhibited an extension moment at the beginning of the impact, which didn't present in the human model. Further investigations are required to explain why this extension/flexion pattern was observed in the physical dummy. Also the current study showed that an increase in impactor speed for the dummy didn't significantly increase the peak flexion moment of the dummy lumbar spine. Based on the above observations, the lumbar flexion moment might not be a good indicator to predict lumbar spine fractures when a H3 dummy used. Secondly, due to the stiffer H3 dummy pelvis design, the impact force and the measured Fz force from the lumbar loadcell were significantly higher than that from the human model and the failure criteria reported from different groups (See Figures. 21a and 21b). A totally redesigned surrogate with better biofidelity of the lumbar and pelvis regions could be more suitable for automotive safety design involving lumbar spine injury prevention.

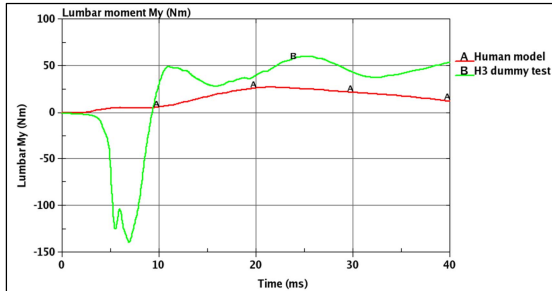


Figure 20. Comparison of the lumbar flexion moment M_y between human model prediction and the H3 dummy test (impact velocity was 7.5m/s).

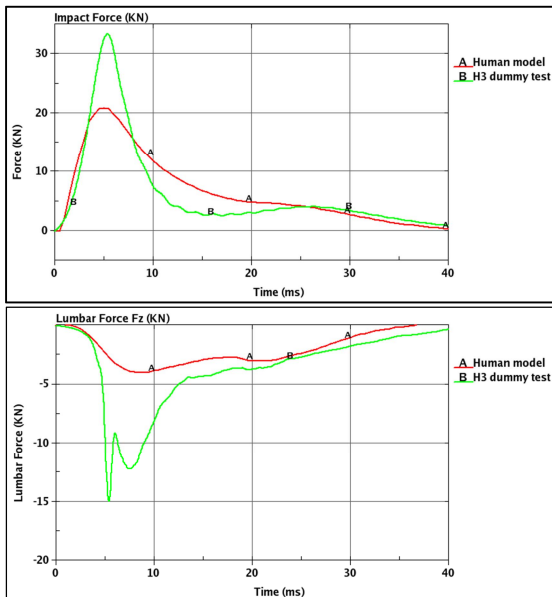


Figure 21. Comparison of the impactor force (a) and the lumbar force F_z (b) between the human model prediction and the H3 dummy test (impact velocity was 7.5m/s).

On the human lumbar fracture threshold impact speed or energy estimation

The element strain based criteria for the lumbar vertebra fractures (see Table 1-2) were validated in this study. However, the definition of “vertebral body fractures” or type of the fractures will affect the threshold impact speed or energy estimation.

For example, from case #6 (Table 9) simulations, we observed that the fractures started from a few cortical bone shell element failure (deletion) and followed sequentially by more cortical shells and trabecular solids failures. Finally the L1 vertebral body collapsed at 15ms and the wedge type fracture was observed (Figure 22 left plot). We

repeated the case#6 run but changed only the impact speed to 9.7 m/s. For this run we observed only a few cortical shell and trabecular solid failures, and no wedge type fracture collapse or large deformation occurred, as shown in Figure 22 on the right plot. If we consider a lumbar fracture as any indication of localized failure of the vertebral body cortical shell(s), the threshold impact speed for the case setup (Figure 4) could be as low as 9.7m/s (or equivalent impact energy of 2070J).

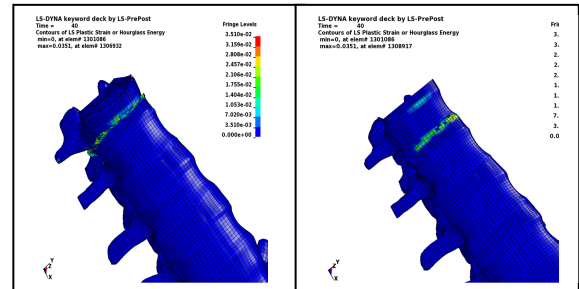


Figure 22. Comparison of the L1 fracture patterns: Left: wedge type fracture at L1 at 10.6m/s impact speed; Right: initial cortical shell failures at L1 at 9.7 m/s impact speed.

Also, in actual impactor testing (Figure 4), the variation of the test configurations or conditions, such as the body supporter block shape and weight, the table material or friction coefficients, and the human body initial positioning, etc., might have influence on the threshold impact speed or energy estimation. We ran additional human body impact test simulations as part of a parametric study on these factors. Table 12 summarizes the simulated test conditions and our observation for initial cortical shell failure at L1 from each of the cases. The two considered human body supporter shapes in these cases were the block that was used in the previous simulation matrix (Table 7, Figure 4) and a wedge shape body supporter shown in Figure 23.

As seen in Table 12, the model predicted that initial cortical shell failure at L1 could occur at a threshold impact speed as low as 8.92m/s (or 1753J impact energy). The most influential factor to affect the threshold impact speed was the body supporter shape or the way we initially positioned the human model. Comparison of run#9 with run#7 showed that the threshold impact speed for L1 cortical shell failure decreased from 9.77 m/s to 8.92 m/s if the body supporter changed from the block to the wedge. The results also indicated that the friction coefficients and the wedge weight under the considered range of 0.92-2.07kg had no

significant effect on the threshold impact speed or energy.

Table 12.
Additional human body impact test simulation cases and results

run#	Pendulum mass(kg)	Impact speed (m/s)	Impact energy (J)	Supporter Shape	Supporter weight (kg)	Wedge/Table Friction Coef.	Local Cortical shell failure?
0	44.05	9.30	1905.1	Wedge	2.073	0.30	YES
1	44.05	9.04	1800.1	Wedge	2.073	0.30	YES
2	44.05	8.92	1752.6	Wedge	2.073	0.30	YES
3	44.05	8.79	1701.9	Wedge	2.073	0.30	NO
4	44.05	8.79	1701.9	Wedge	0.924	0.80	NO
4b	44.05	8.92	1752.6	Wedge	0.924	0.80	YES
5	44.05	8.79	1701.9	Wedge	0.924	0.55	NO
6	44.05	8.79	1701.9	Wedge	0.924	0.30	NO
7	44.05	8.92	1752.6	Wedge	0.924	0.30	YES
8	44.05	9.05	1804.1	Wedge	0.924	0.30	YES
9	44.05	9.77	2102.6	Block	0.924	0.30	YES
10	44.05	9.05	1804.1	Block	0.924	0.30	NO

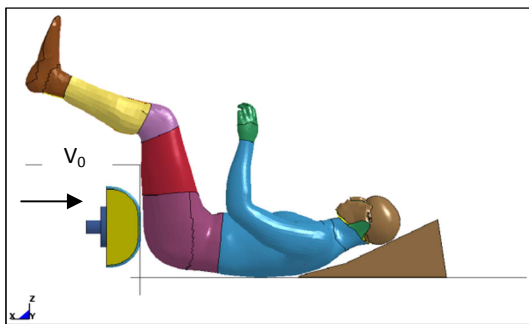


Figure 23. Alternate Linear Impactor test setup for the full human body model.

CONCLUSIONS

A full body human model with a detailed representation of the anatomical structures of the lumbar spine, and with the validated tissue-level injury criteria for the lumbar vertebral fractures under compressive-dominated loadings has been developed.

A linear impactor test configuration shown in Figure 4 was used for comparative study of lumbar loads response between the human full body model and the Hybrid-III 50thtile dummy. The results showed that the threshold impactor velocities at which the lumbar vertebrae fracture at L1 occurred were in the range of 8.92-10.6m/s of impact speeds (or 1750-2475J of impact energies). Localized cortical shell failures were observed starting from the lower threshold impact velocity of 8.92 m/s. The wedge type vertebrae fractures at the L1 level occurred at 10.6m/s. The human body supporter shape in this test setup was found to have the most significant effect on the threshold impact velocity or energy.

Physical lab impactor tests in the same test setup configuration were run for the Hybrid-III 50thtile dummy at multiple impact speeds in the range of 5.5m/s-7.5m/s. The test data showed that the dummy lumbar load Fz reached 14.5 KN at the 7.5m/s impact. Differences of the lumbar loads between the human body and the H3 50thtile dummy have been identified from this study.

ACKNOWLEDGEMENT

The authors would like to gratefully acknowledge to Richard Kent, Damien Subit and Zuoping Li of University of Virginia for their support in development work of Takata Human Model v4.0 used in this study. Also thanks to Albert King of Wayne State University for his providing us information of the PMHS vertical sled test data for the model correlation.

REFERENCES

- Ashton-Miller and Schultz, "Biomechanics of Human Spine", Basic Orthopaedic Biomechanics, 2nd ed. edited by VC. Mow and WC Hayes. Lippincott-Raven, Philadelphia, PA, pp. 353-394, 1997.
- Backaitis SH and Mertz HJ., "Hybrid III: The First Human-Like Crash Test Dummy" SAE, Warrendale, PA, 1994.
- Baudrit, P. et al., "Cadaver and Dummy Investigation of Injury Risk with Anti-Sliding System In Case of Static Deployment" ESV paper #05-0399, 2005.
- Belwadi, A. and Yang, K.H., "Cadaveric Lumbar Spine Responses to Flexion with and without Anterior Shear Displacement", IRCOBI Conference, Bern, Switzerland, 2008.
- Demetropoulos, C.K., Yang, K.H., Grimm, M.J., Khalil, T.B., King, A.I.; "Mechanical Properties of the Cadaveric and Hybrid III Lumbar Spines", 42nd Stapp Car Crash Conference, Paper No. 983160, 1998.
- F. Pintar, "Thoraco-Lumbar Spine fractures in Frontal Impacts", 2012 CIREN Conference Presentation, 2012a.
- F. Pintar, "Spine and Pelvis Fractures in Axial Z-Acceleration", 40th International Workshop on

Human Subjects for Biomechanics Research”, 2012b.

Jakobsson L, Bergman T, and Johansson L., “Identifying Thoracic and Lumbar Spinal Injuries in Car Accidents”, IRCOBI Conference, Madrid, Spain, p61-71, 2006.

King AI., and Vulcan AP., “Elastic Deformation Characteristics of the Spine” J. Biomech. Vol 4. pp. 413-429, 1971.

Matthew W. Kindig, et al., “Structural Response of Cadaveric Ribcages Under a Localized Loading: Stiffness and Kinematic Trends”, Stapp 2010-22-0015, 2010.

Nahum AM and Melvin JW, “Accidental Injury, Biomechanics and Prevention.” Springer-Verlag, New York, USA, 1993.

Prasad P., “The Dynamic Response of the Spine During +Gz (Eyeballs Down) Acceleration.” Ph. D. dissertation, Wayne State University, Detroit, MI, 1973.

Greg Shaw, et al, “Impact Response of Restrained PMHS in Frontal Sled Tests: Skeletal Deformation Patterns under Seat Belt Loading”, Stapp Car Crash Journal, 2009-22-0001, 2009.

Yoganandan, N., Myklebust, J.B., Cusick, J.F., Wilson, C.R., Sances, A.; “Functional biomechanics of the thoracolumbar vertebral cortex”, Clinical Biomechanics, 3:11-18, 1988a.

Yoganandan, N., Pintar, F., Sances, A. Jr., Maiman, D., Myklebust, J., Harris, G., Ray, G.; “Biomechanical Investigations of the Human Thoracolumbar Spine”, SAE Technical Paper 881331, 1988b.

Zhao, Jay and Narwani, G., “Biomechanical Analysis of Hard Tissue Responses and Injuries with Finite Element Full Human Body Model.” ESV 07-0354, 2007.